

## Article

# An Improved DPSIR-DEA Assessment Model for Urban Resilience: A Case Study of 105 Large Cities in China

Liudan Jiao <sup>1,\*</sup>, Bowei Han <sup>1</sup>, Qilin Tan <sup>1</sup>, Yu Zhang <sup>1</sup>, Xiaosen Huo <sup>1</sup>, Liu Wu <sup>1</sup> and Ya Wu <sup>2</sup>

<sup>1</sup> School of Economics and Management, Chongqing Jiaotong University, Chongqing 400074, China; hbw@mails.cqjtu.edu.cn (B.H.); tanqilin@mails.cqjtu.edu.cn (Q.T.); yuzhang@cqjtu.edu.cn (Y.Z.); huoxiaosen@cqjtu.edu.cn (X.H.); 990202200030@cqjtu.edu.cn (L.W.)

<sup>2</sup> College of Resources and Environment, Southwest University, Chongqing 400715, China; mswuya@swu.edu.cn

\* Correspondence: jld@cqjtu.edu.cn

**Abstract:** Urban development is facing increasingly complex disturbances. Assessing large cities' urban resilience is important for improving their ability to withstand disturbances and promoting sustainable development. Therefore, this paper establishes an improved assessment model for urban resilience based on the driving force–pressure–state–impact–response (DPSIR) and data envelopment analysis (DEA) model. The Malmquist index, Dagum Gini coefficient, and Markov chain were sequentially used for spatiotemporal evolution and differential resilience analysis. Then, 105 large Chinese cities were selected as case studies. The results indicate their overall resilience is relatively high; each year's average resilience efficiency can achieve DEA effectiveness. The distribution pattern of resilience level presents a healthy olive-shaped structure. However, there is also a significant difference between the two poles. During the research period, the combined effect of technological efficiency improvement and technological progress resulted in the overall resilience slowly improving, and this process was more driven by technological innovation. At the same time, the overall regional difference in resilience also shows a narrowing trend, and the current spatial differences mainly come from the difference within subregions and super-density. In future transfer predictions, the resilience of large cities will show good stability with a higher probability of maintaining stability; if the resilience undergoes a transition, the probability of an increase will be higher than a decrease. Based on the life cycle process of resilience, this study selects indicators that can characterize the level of resilience according to the DPSIR model, which comprehensively reflects the characteristics of urban resilience. This study's results can provide particular reference values for urban disaster response emergency planning and sustainable development construction, and it also provides new ideas for the assessment research of urban resilience.

**Keywords:** urban resilience; DPSIR-DEA model; assessment model; Dagum Gini coefficient



**Citation:** Jiao, L.; Han, B.; Tan, Q.; Zhang, Y.; Huo, X.; Wu, L.; Wu, Y. An Improved DPSIR-DEA Assessment Model for Urban Resilience: A Case Study of 105 Large Cities in China. *Land* **2024**, *13*, 1133. <https://doi.org/10.3390/land13081133>

Academic Editors: Hossein Azadi and André Samora-Arvela

Received: 27 June 2024

Revised: 23 July 2024

Accepted: 23 July 2024

Published: 25 July 2024



**Copyright:** © 2024 by the authors. Licensee MDPI, Basel, Switzerland. This article is an open access article distributed under the terms and conditions of the Creative Commons Attribution (CC BY) license (<https://creativecommons.org/licenses/by/4.0/>).

## 1. Introduction

With the gradual acceleration of global urbanization, large-scale population aggregation has brought vitality to the development of cities. However, it has also significantly increased the pressure on various cities' infrastructures. The capability of infrastructure is complex to match the population's needs, which has brought a series of potential crises to rapidly developing cities [1]. At the same time, due to the environmental damage caused by modern human activities, extreme weather has occurred frequently. For example, Henan Province in China was hit by a hefty rainstorm in July 2021, which affected 14.78 million people. The negative consequences caused by rapid urbanization and frequent natural disasters seriously hinder the normal development of cities, directly promoting urban resilience research [2]. Some scholars pointed out that the different abilities of cities to cope with external risks stem from the difference in their resilience [3]. Resilience refers to the

ability of a system to absorb risks to the maximum extent, maintain its original functional stability, and gradually adapt to risks when facing external shocks [4]. The higher the level of resilience, the greater the system's ability to resist external disturbances. The United Nations Human Settlements Programme pointed out that urban resilience construction should be a critical global agenda [5]. Therefore, measuring urban resilience is significant for promoting high-quality urban development.

Meanwhile, cities with populations exceeding 1 million or even 10 million have gradually emerged worldwide. For example, Tokyo is one of the world's most populous and urbanized cities, reaching about 38 million people in 2022 [6]. New Delhi, Shanghai, and São Paulo are mega cities with populations of over 20 million people. By the end of 2020, there were 532 cities worldwide with a population of over one million. The Chinese government defined a large city as one with a permanent population of over 1 million people in urban areas. By 2022, China already had 105 large cities. Compared with ordinary cities, large cities are usually the central cities within a specific area, with a larger population and more important political and economic status. Various complex urban activities and the interaction between cities are becoming increasingly frequent, increasing the importance of large cities daily. However, the inability of infrastructure to meet the population's needs and the increasing environmental damage have brought various pressures to the resilience of large cities. Therefore, it is necessary to accelerate the research on the resilience of large cities to improve their stability. Some scholars have noticed this issue and begun to explore the urban planning [7] and disaster resistance capabilities [8] of some large cities.

Resilience was initially applied in engineering to describe the stability of materials and their performance in restoring their original state under external forces [9]. Recently, resilience theories have been applied in urban research. Scholars have engaged in heated discussions on the connotation of urban resilience [10]. For example, Zhang et al. [11] define urban resilience as the ability of urban systems to cope with uncertainties such as external disturbances or long-term changes, emphasizing the self-organizing processes of cities in the face of disasters, including absorbing losses and gradually adapting to risks. Vargas et al. [12] define urban resilience as the ability of the social ecosystem extended by a city to maintain essential structural functions in the event of disturbances.

In order to better determine the ability of cities to cope with external risks and more accurately evaluate the level of urban resilience, scholars have conducted studies on establishing an evaluation index system for urban resilience. The overall impact of urban subsystems such as the economy, society, and infrastructure [13] on urban resilience is mainly based on urban characteristics and elements. For example, Xun et al. [14] constructed an urban resilience evaluation index system based on dimensions such as economy, society, ecological environment, and municipal facilities. Some studies analyze the resilience process in response to external risks in cities, including the stages of pre-disaster warning, disaster resistance, post-disaster recovery, and adaptation that cities experience when disasters invade cities [15]. Selecting indicators based on urban behaviors at different stages can more accurately reflect the role of urban resilience in risk impact. For example, Zhang et al. [16] developed a comprehensive flood resilience assessment framework based on the pressure–state–response (PSR) model, which can systematically evaluate the performance of cities in flood disasters. Ji et al. [17] applied the PSR model to study the resilience of floods from the pressure caused by disaster factors to the urban state during disasters and then to the post-disaster urban recovery and resilience improvement.

Resilience evaluation mainly relies on various quantitative evaluation methods. Most studies adopt a comprehensive weighting method that combines weighting and quantitative analysis [18]. For example, Moghadas et al. [19] applied the analytic hierarchy process (AHP) and technique for order preference by similarity to an ideal solution (TOPSIS) model to evaluate Tehran, Iran's flood disaster resistance capacity. This method is limited to relying on a subjective weighting process. Therefore, objective weights such as the entropy weighting method are often used to avoid subjective errors. Zhou et al. [20] comprehensively applied the TOPSIS, entropy weight method, and coupling coordination model

to evaluate the resilience of six cities along the Sichuan–Tibet Railway in China. Some studies have attempted to introduce more ideas for urban resilience assessment, including image analysis using radar images [21], comprehensive models based on geographic information systems and AHP [22], and hybrid methods combining network analysis and decision-making experiments [23].

Based on the above discussion, it can be found that scholars have begun to pay attention to the resilience of large cities. However, the existing research on establishing an evaluation index system lacks the combination of urban resilience characteristics and rarely pays attention to the balance of internal subsystems of resilience while evaluating resilience levels. Meanwhile, the emphasis is only on the balance of subsystems while neglecting efficiency. In that case, it will significantly affect the construction of urban resilience [24]. The driving force–pressure–state–impact–response (DPSIR) model has been widely used in evaluating complex systems due to its comprehensiveness, holism, and flexibility. It can fully characterize the relationships between various elements through causal chains and effectively evaluate the proper level of the target object. This model is based on complete logical relationships that could evaluate system changes' causes, processes, and consequences [25]. Structural checks can also be provided during the evaluation process, and feedback can be provided promptly [26]. In addition, the data envelopment analysis (DEA) model can meet the efficiency evaluation with multiple input–output units without the need to determine indicators' weights, and the evaluation results are objective and accurate. Hence, they are especially suitable for the evaluation research of complex systems such as cities [27]. Therefore, this study attempts to analyze the resilience process and explore the characteristics of urban resilience based on the balanced perspective of internal subsystems, aiming to construct an urban resilience assessment model with an integrated perspective and comprehensive elements. This research will select evaluation indicators based on the DPSIR model that fit the characteristics of the resilience stage, Define the input–output properties of resilience elements in combination with the DEA model, leverage the advantages of the DEA model that does not require determining indicator's weights and can handle multiple input–output elements, ultimately establish an objective and effective urban resilience evaluation indicator system. Selecting 105 large cities in China for a case study, the research object covers cities from all directions, types, and grades in China, analyzing the distribution and dynamic evolution of their resilience from 2017 to 2021. Finally, further study of dynamic evolution and difference analysis using the Malmquist index, Dagum Gini coefficient, and Markov chain propose reasonable suggestions based on the shortcomings of current resilience construction, which can obtain more universal resilience development laws.

The contributions of this paper are as follows: (1) under the guidance of urban resilience theory, based on the DPSIR model, indicators were selected from the five dimensions of “driving force–pressure–state–impact–response” to construct an urban resilience evaluation index system that reflects the process of resilience; (2) based on the resilience evaluation index system, DEA model was used to measure the resilience level and establish an efficient and accurate urban resilience assessment model; and (3) this study analyzes the dynamic evolution and spatiotemporal characteristics of urban resilience using the Malmquist index, Dagum Gini coefficient, and Markov chain.

## 2. The Development of the Assessment Model for Urban Resilience

This study establishes an urban resilience assessment model for large cities based on the DPSIR-DEA model, and its framework is shown in Figure 1.

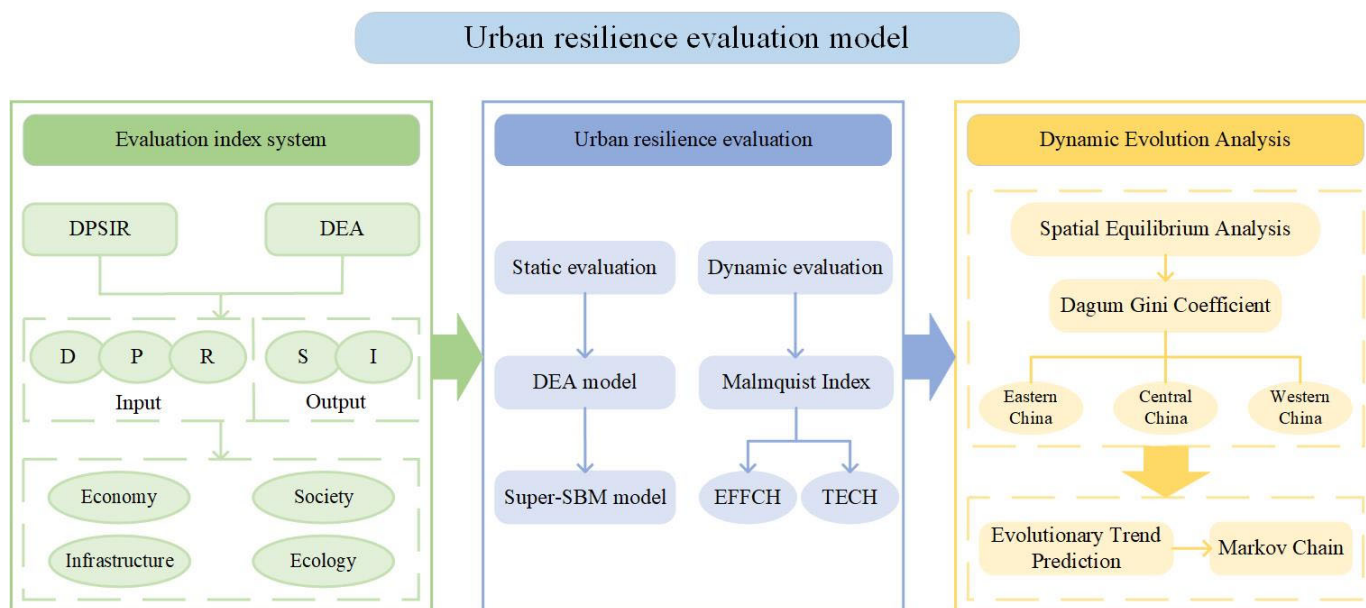


**Figure 1.** The structural framework of the model.

## 2.1. Establishment of the Urban Resilience Evaluation Index System

### 2.1.1. DPSIR Model

The DPSIR model is an evaluation model proposed by the European Environment Agency that reflects the causal relationship between human activities and the environment [28]. It is widely used to evaluate the internal logic and impact relationships among multiple factors [29]. The DPSIR model provides an analytical framework that divides the evaluation indicators into five dimensions: ‘driving force’, ‘pressure’, ‘state’, ‘impact’, and ‘response’. It can capture the logical relationships between various elements [30] and achieve the integration of human activities, socio-economic factors, and the ecological environment into a complete system [31]. Importantly, it can provide a detailed description of the unity and opposition between various elements while analyzing the limiting factors from a causal and relational perspective.

By analyzing the characteristics and behavioral patterns of the DPSIR model, it can be found that its application in urban resilience is consistent with the resilience characteristics. It can be combined with urban disaster response, disaster resistance, and post-disaster recovery [32]. Moreover, as urban resilience is a complex system composed of multiple subsystems, each subsystem also contains various functional elements, so any change in these elements will affect the remaining elements’ stability. Therefore, when evaluating urban resilience, if we want to analyze its mechanism further, there is a need for a comprehensive and logical model. Commonly logical models include PSR and driving force–state–response (DSR) models [32]. However, they have limitations, such as limited dimensions and insufficient analysis of dynamic mechanisms, which cannot accurately present the process of resilience improvement. The DPSIR model is obtained by optimizing the PSR and DSR models. It compensates for the two models’ respective shortcomings. It adds a new dimension, ‘impact’, further enriching the model’s logic.

In the DPSIR model, the five subsystems of driving force, pressure, state, impact, and response are connected through the chain of transmitting information and data [33]. Based on the characteristics of the DPSIR model and its application in urban resilience, this article designs a framework as shown in Figure 2.

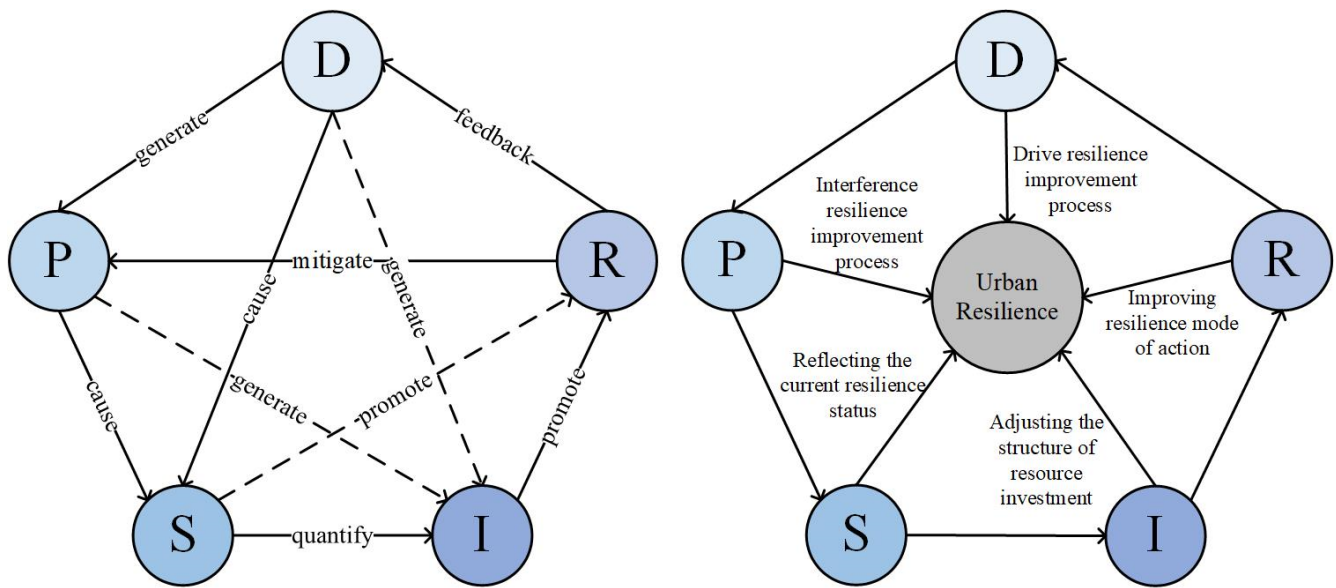


**Figure 2.** DPSIR model and its application in urban resilience.

In Figure 2, the dimensions of the DPSIR model are interrelated, with solid lines indicating direct connections and dashed lines indicating indirect connections. In applying the DPSIR model to urban resilience, the driving force (D) is the fundamental force that starts the resilience process, including factors that trigger risk changes and change stable states, such as socio-economic development. Due to changes in the driving force, the original stable state of the system and cities may be affected by various interferences, resulting in pressure (P). State (S) refers to a city’s state after being simultaneously driven by the driving force and pressure. It should be able to reflect the level of urban development intuitively and the residents’ living conditions and, to some extent, evaluate the city’s ability to recover to its original level in resilient disturbances. The state changes impact society and the ecological environment (I), which can evaluate resilience and adjust the resource investment structure based on the results. Response (R) refers to the system’s attempt to improve urban resilience by summarizing experience and optimizing the resilience mode [34,35].

### 2.1.2. DPSIR-DEA Model

As a complex coupled system, urban resilience has numerous evaluation indicators and a large amount of data, making its evaluation difficult. The currently widely used evaluation models, including the TOPSIS model [20], mostly require weighting or data processing, which inevitably leads to errors and makes it difficult to obtain accurate evaluation results. However, the advantage of the DEA model is that it precisely meets the complex systems’ requirements. It distinguishes the nature of indicators into input and output, obtains evaluation results based on raw data, avoids the interference of errors in the evaluation process, and has the advantages of high efficiency and accuracy. The DEA model can handle complex practical problems without strict parameter limitations and is a powerful tool for evaluating and improving the performance of decision units.

Based on the DEA model, it is necessary to define the properties of the DPSIR model’s subsystem to distinguish the input–output properties of factors. The initial stage combines urban resilience characteristics, driving forces, and pressure subsystems. Many investments are required to promote the beginning of the resilience process. Therefore, they belong to input indicators. State and Impact subsystems that reflect infrastructure, economic, and social levels can evaluate the final results of resilience construction, so they should belong to output indicators. The response subsystem is the final stage. It uses measures such as adjusting resource investment structure or optimizing resilience improvement strategies to

improve resilience. Therefore, it also belongs to the input indicator. The DPSIR-DEA model is shown in Figure 3:

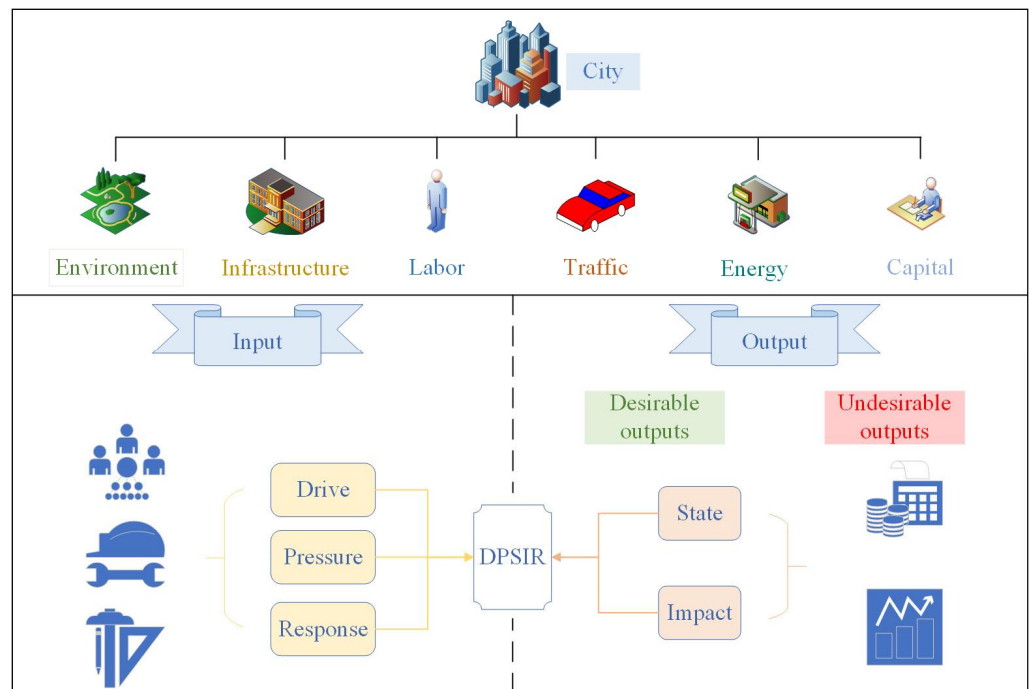


Figure 3. DPSIR-DEA model.

In order to demonstrate the spatiotemporal dynamics of the DPSIR model, its circular structure is further decomposed into linear structures and arranged in order of multiple stages [30], as shown in Figure 4. During the response phase, while providing feedback on the results of this stage, it can also summarize the experience and promote the start of the next resilience stage. Therefore, resilience construction is a cyclical process, and the resilience level can be improved to a certain extent after each complete stage.

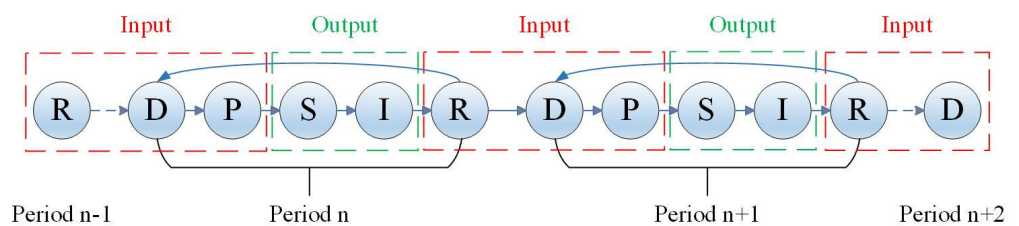


Figure 4. Multi-stage DPSIR-DEA model.

### 2.1.3. Urban Resilience Evaluation Index System

The various urban elements and subsystems are closely connected, and urban resilience emphasizes coordination. Therefore, this study establishes an evaluation index system based on the DPSIR-DEA model. Indicators reflecting the process of resilience improvement are selected, and their input–output properties are defined according to the DEA model. Finally, four elements, including economy, society, ecology, and infrastructure, are selected based on the definition and analysis of each dimension of the DPSIR model in the previous. The detailed indicators are shown in Table 1.

Table 1. Urban resilience evaluation index system.

Property Layer	Criterion Layer	Element Layer	Index Layer	Unit	Reference
Input	Driving force	Economy	Proportion of the tertiary industry	%	[8,20]
			General public budget revenue	Ten thousand yuan	[8,36]
		Society	Urbanization rate	%	[20,37]
			Built-up Area	Square Kilometer	[2,38]
		Infrastructure	Number of hospitals	Piece	[1,36]
			Per capita road area	Square meter	[18,39]
Input	Pressure	Economy	GDP growth rate	%	[1,20]
			Growth rate of fixed assets investment	%	[17,20]
		Society	Total electricity consumption	10,000 kWh	[1,18]
			Total natural gas supply	10,000 cubic meters	[3,32]
		Infrastructure	Drainage pipeline length	kilometer	[17,20]
			Number of beds	Piece	[17,39]
Output	State	Society	Urban unemployment rate	%	[8,35]
			Per capita park green space area	Square meter	[8,20]
		Infrastructure	Number of universities	Piece	[15,32]
			Total sulfur dioxide emissions	ton	[8,36]
		Ecology	The total amount of industrial wastewater discharge	10,000 tons	[18,32]
			Number of urban employees purchasing medical insurance	Person	[8,36]
Output	Impact	Society	Per capita disposable income of urban residents	Yuan	[20,38]
			Harmless treatment rate of household waste	%	[20,32]
		Infrastructure	Centralized sewage treatment rate	%	[8,36]
			Greening rate in built-up areas	%	[8,20]
			Economy	Expenditure on education	10,000 yuan
Input	Response	Society	Expenditure on R&D	10,000 yuan	[18,36]

#### 2.1.4. Study Area and Data Sources

By 2022, there were 105 large cities in China with a permanent population of over 1 million people in urban areas, and this study selected them as the research objects. Their locations are marked in Figure 5. In order to identify their geographical characteristics and conduct subsequent research, this article distinguishes the eastern, central, and western regions to which they belong. Since some cities had not released partial indicator data for 2022, based on the principles of accuracy and scientific, this study set the research period from 2017 to 2021. The research data were collected from the Statistical Yearbook, Urban Construction Statistical Yearbook, and National Economic and Social Development Statistical Bulletin of various cities.

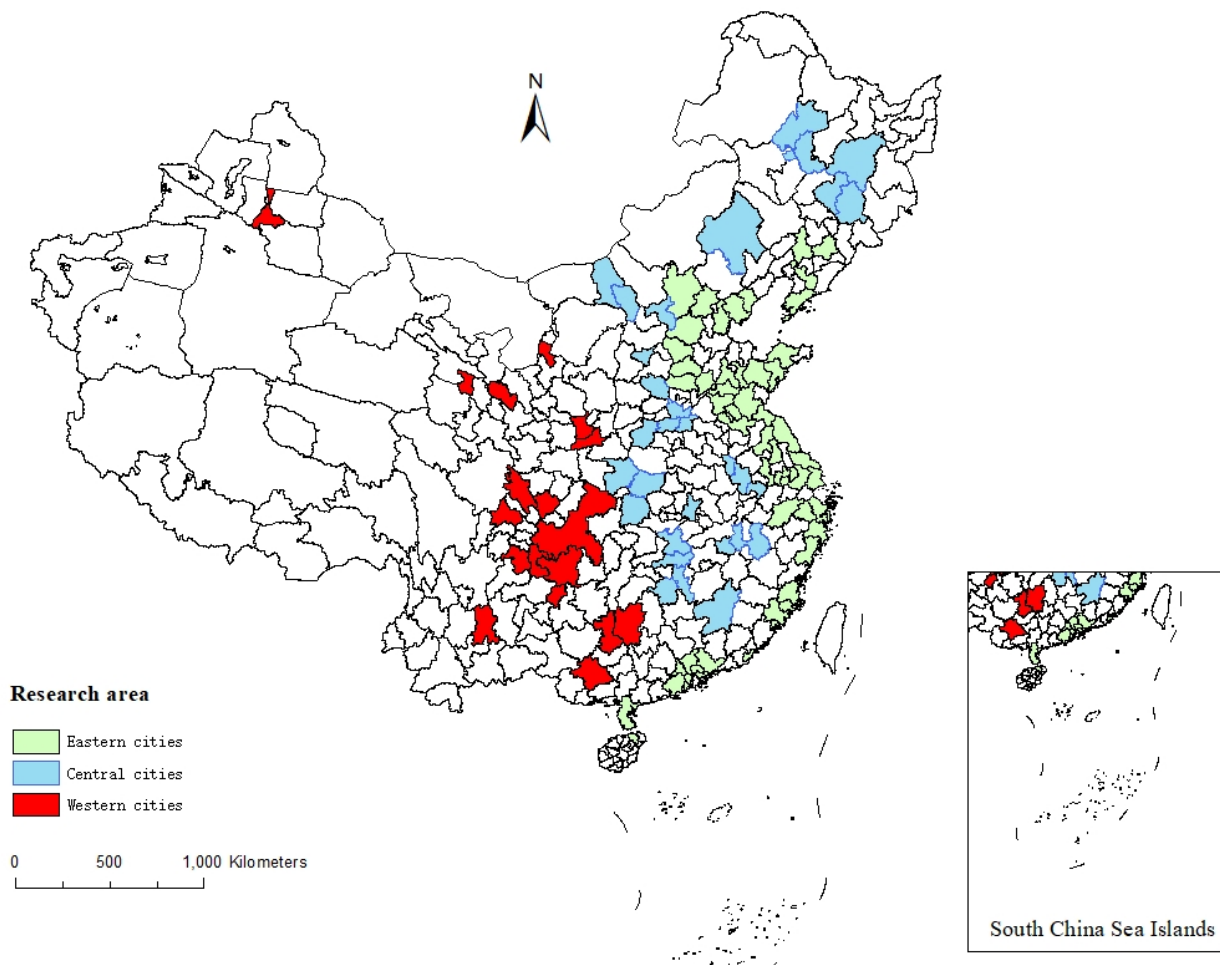


Figure 5. Research area.

### 2.2. Measurement of Urban Resilience Level Based on DEA

This study chose the DEA model to evaluate resilience. The DEA model is suitable for evaluating the relative efficiency between multiple input–output units. It does not require assuming the form of production functions in advance, setting indicator weights, or standardizing the original data, which can avoid the influence of subjective factors [40]. It is widely used in efficiency evaluation in various industries [41]. However, traditional DEA models cannot evaluate units with an efficiency value of 1. They assume all system outputs are valuable, ignoring unexpected outputs that can significantly impact efficiency results. Later, Tone proposed a Super-Slack-Based Measure (Super-SBM) model that solved the problem of input–output relaxation by incorporating relaxation variables into the objective function, making it an essential method for measuring development efficiency [42]. It can evaluate units with an efficiency value of 1, provide a more accurate and comprehensive efficiency analysis, and provide a framework for sorting effective units [43]. Therefore, this study used the Super-SBM model to evaluate urban resilience. The formulas are as follows:

Firstly, determine the input–output matrix. Assuming there are  $n$  cities, equivalent to  $n$  decision-making units (DMUs), each with  $m$  inputs,  $q_1$  expected outputs and  $q_2$  unexpected outputs, which are successively represented by matrices  $X$ ,  $Y^s$ ,  $Y^b$ :

$$X = [x_1, \dots, x_n] \in R^{m \times n} > 0 \tag{1}$$

$$Y^s = [y_1^s, \dots, y_n^s] \in R^{q_1 \times n} > 0 \tag{2}$$

$$Y^b = [y_1^b, \dots, y_n^b] \in R^{q_2 \times n} > 0 \tag{3}$$

Then, the resilience efficiency of city  $k$  is obtained through the Super-SBM model, as shown in Table 2.

**Table 2.** Formulas for the Super-SBM model.

Attribute	Abbreviation	Formula	Number
Set of production possibilities	$p$	$\left\{ (x, y^g, y^b) \mid x \geq X\lambda, y^g \leq Y^g\lambda, y^b \leq Y^b\lambda, \lambda \geq 0 \right\}$	(4)
Constant returns to scale (CRS)	$\lambda$	Non-negative intensity vector	
Efficiency value	$\rho$	$\min \rho = \frac{1 + \frac{1}{m} \sum_{i=1}^m s_i^- / x_{ik}}{1 - \frac{1}{q_1 + q_2} \left( \sum_{r=1}^{q_1} s_r^+ / y_{rk}^g + \sum_{t=1}^{q_2} s_t^{b-} / y_{tk}^b \right)}$	(5)
Slack variables of input	$s_i^-$	$\sum_{j=1}^n \lambda_j x_{ij} - s_i^- \leq x_{ik} \quad (i = 1, 2, \dots, m)$	(6)
Expected output	$s_r^+$	$\sum_{j=1}^n \lambda_j y_{rj}^g + s_r^+ \geq y_{rk}^g \quad (r = 1, 2, \dots, q_1)$	(7)
Unexpected output	$s_t^{b-}$	$\sum_{j=1}^n \lambda_j y_{tj}^b - s_t^{b-} \leq y_{tk}^b \quad (t = 1, 2, \dots, q_2)$	(8)
		$1 - \frac{1}{q_1 + q_2} \left( \sum_{r=1}^{q_1} s_r^+ / y_{rk}^g + \sum_{t=1}^{q_2} s_t^{b-} / y_{tk}^b \right) > 0$	(9)
		$\lambda_j, s_i^-, s_r^+, s_t^{b-} \geq 0, j = 1, 2, \dots, n (j \neq k)$	(10)

When  $\rho \geq 0$ , DMU is considered DEA valid, and the higher the value of  $\rho$ , the higher the resilience level of the city; When  $\rho < 0$ , DMU is DEA invalid.

Based on the efficiency calculation results, the natural fracture point method can be used to classify the resilience of cities into five levels: high resilience, medium-high resilience, medium resilience, medium-low resilience, and low resilience.

### 2.3. Dynamic Level Evaluation of Urban Resilience Based on the Malmquist Index

The Super-SBM model can only measure the static level of urban resilience and cannot reflect the change process of resilience in a time series [44]. In order to compensate for its lack of dynamism, this paper introduces the Malmquist index to measure the change in urban resilience during the research period. The Malmquist index was established by Caves et al., which initially calculated changes in productivity. It gradually combined with DEA theory to become an important method for measuring efficiency changes in adjacent periods of a region [45]. Since the Malmquist index can not only track the changes in resilience efficiency over a while but also further analyze the reasons for efficiency changes based on its decomposition index [46], it is currently widely used in the dynamic evolution research of efficiency in various fields [47].

Malmquist index is defined based on benchmark techniques. Therefore, based on the efficiency value  $\rho$  of period  $t$ , the Malmquist indexes for the changes in resilience efficiency during period  $t$  and  $t + 1$  are as follows:

$$M^t = \rho^t(x^{t+1}, y^{t+1}) \mid \rho^t(x^t, y^t) \tag{11}$$

$$M^{t+1} = \rho^{t+1}(x^{t+1}, y^{t+1}) \mid \rho^{t+1}(x^t, y^t) \tag{12}$$

Take the  $j$ th city as an example. The Malmquist index can be obtained from the geometric mean of the two Malmquist indexes mentioned above, which serve as a measure of the change in total factor productivity from period  $t$  to  $t + 1$ :

$$M_j(x^t, y^t, x^{t+1}, y^{t+1}) = \sqrt{\frac{\rho_j^t(x^{t+1}, y^{t+1})}{\rho_j^t(x^t, y^t)} \times \frac{\rho_j^{t+1}(x^{t+1}, y^{t+1})}{\rho_j^{t+1}(x^t, y^t)}} = TFPCH \tag{13}$$

Furthermore, Fare et al. decomposed the Malmquist index into technical change (TECH) and technical efficiency change (EFFCH) based on the premise of constant returns to scale (CRS), as shown in Table 3.

**Table 3.** Decomposed Maimquist index.

Abbreviation	Formula	Number
	$EFFCH \times TECH$	(14)
$TFPCH$	$\frac{\rho_j^{t+1}(x^{t+1}, y^{t+1})}{\rho_j^t(x^t, y^t)} \times \sqrt{\frac{\rho_j^t(x^{t+1}, y^{t+1})}{\rho_j^{t+1}(x^{t+1}, y^{t+1})} \times \frac{\rho_j^t(x^t, y^t)}{\rho_j^{t+1}(x^t, y^t)}}$	(15)
$EFFCH$	$\frac{\rho_j^{t+1}(x^{t+1}, y^{t+1})}{\rho_j^t(x^t, y^t)}$	(16)
$TECH$	$\sqrt{\frac{\rho_j^t(x^{t+1}, y^{t+1})}{\rho_j^{t+1}(x^{t+1}, y^{t+1})} \times \frac{\rho_j^t(x^t, y^t)}{\rho_j^{t+1}(x^t, y^t)}}$	(17)

By analyzing the formulas in Table 3, when  $TFPCH > 1$ , the Malmquist index is greater than 1, it indicates that the total factor productivity from period  $t$  to  $t + 1$  shows a positive growth and productivity improvement [48]. When  $TFPCH \leq 1$ , productivity remains unchanged or decreases. When  $TECH > 1$ , the production front is moving outward, and technological innovation is making progress. When  $TECH = 1$ , the production front has not moved, and the production technology has not changed. When  $TECH < 1$ , the production front is moving backward, and the technology has regressed. When  $EFFCH > 1$ , it indicates an improvement in technical efficiency and a narrowing of the gap between the decision-making unit and efficiency frontier. When  $EFFCH = 1$ , the technical efficiency of two adjacent periods is the same. When  $EFFCH < 1$ , it indicates a decrease in technical efficiency and an increase in the gap between the decision-making unit and efficiency frontier.

**2.4. Spatial Equilibrium Analysis of Urban Resilience Based on Dagum Gini Coefficient**

The Gini coefficient is mainly used to reflect the overall balance of a region because it can characterize the degree of spatial imbalance of variables. However, this method is limited to a holistic perspective. It cannot further decompose regional disparities, making it difficult to describe the balance of each subregion and determine the source of differences. To solve this problem, Dagum proposed a new approach that divides the Gini coefficient into three components: the contribution of the gap within the subregion ( $G_w$ ), the contribution of the super variable net value gap between subregions ( $G_{nb}$ ), and the contribution of the super variable density between subregions ( $G_t$ ). The decomposed variables satisfy the relationship formula:

$$G = G_w + G_{nb} + G_t \tag{18}$$

The decomposed Gini coefficient can reflect the degree of balance in subregions and analyze the sources of difference by comparing the contribution level of three variables. Therefore, this method is widely used to study regional differences [49–51], and this study uses it to analyze regional differences in resilience. Its research formulas are as follows [52]:

$$G = \frac{\sum_{j=1}^k \sum_{h=1}^k \sum_{i=1}^{n_j} \sum_{r=1}^{n_h} |\rho_{ji} - \rho_{hr}|}{2n^2\bar{\rho}} \tag{19}$$

$$\bar{\rho} = \sum_{j=1}^k \sum_{i=1}^{n_j} \frac{\rho_{ji}}{n} \tag{20}$$

In the above formulas,  $G$  is the overall Gini coefficient, and the smaller its value, the higher the level of resilience spatial equilibrium in the study area;  $\bar{\rho}$  is the average resilience level of all cities;  $n$  represents the total number of cities in the study area; and  $k$  is the number of subregions. Taking subregion  $j$  as an example, the number of cities within it

is  $n_j$ , and the resilience level of the  $i$ -th city is recorded as  $\rho_{ji}$  ( $j = 1, 2, 3; i = 1, 2, \dots, n_j$ ); Subregion  $h$  is the same,  $h = 1, 2, 3; r = 1, 2, \dots, n_h$ .

$$\bar{\rho}_h \leq \dots \bar{\rho}_j \leq \dots \bar{\rho}_k \tag{21}$$

When decomposing the Gini coefficient, the average resilience of each subregion should be ranked first, where  $\bar{\rho}_j = \sum_{i=1}^{n_j} \frac{\rho_{ji}}{n_j}$ . Then, calculate each decomposition part using the formulas in Table 4.

**Table 4.** Related parameters of Gini coefficient.

Attribute	Abbreviation	Formula	Number
Gini coefficient of subregion $j$	$G_{jj}$	$\frac{\frac{1}{2n_j^2} \sum_{i=1}^{n_j} \sum_{r=1}^{n_j}  \rho_{ji} - \rho_{jr} }{n_j^2}$	(22)
	$G_w$	$\sum_{j=1}^k G_{jj} p_j s_j$	(23)
Extended Gini coefficient between subregion $j$ and $h$	$G_{jh}$	$\frac{\sum_{i=1}^{n_j} \sum_{r=1}^{n_h}  \rho_{ji} - \rho_{hr} }{n_j n_h (\bar{\rho}_j + \bar{\rho}_h)}$	(24)
	$G_{nb}$	$\sum_{j=2}^k \sum_{h=1}^{j-1} G_{jh} (p_j s_h + p_h s_j) D_{jh}$	(25)
	$G_t$	$\sum_{j=2}^k \sum_{h=1}^{j-1} G_{jh} (p_j s_h + p_h s_j) (1 - D_{jh})$	(26)
Relative impact of unit resilience levels between subregion $j$ and $h$	$D_{jh}$	$\frac{d_{jh} - p_{jh}}{d_{jh} + p_{jh}}$	(27)
Proportion of cities in subregion $j$	$p_j$	$\frac{n_j}{n}$	(28)
Proportion of total urban resilience efficiency in subregion $j$	$s_j$	$\frac{n_j \bar{\rho}_j}{n \bar{\rho}}$	(29)
	$d_{jh}$	$\int_0^\infty dF_j(\rho) \int_0^\rho (\rho - x) dF_h(x)$	(30)
	$p_{jh}$	$\int_0^\infty dF_h(\rho) \int_0^\rho (\rho - x) dF_j(\rho)$	(31)

### 2.5. Dynamic Evolution Analysis of Urban Resilience Based on Markov Chain

In order to achieve dynamic development prediction of resilience, this study introduced the Markov chain. Markov chain is a random prediction model that can predict the probability of a target transitioning from one state to another under the given historical data of a time series and consider the resilience changes in different periods [53]. Therefore, its results depend on the probability of state transition. This study introduced a state transition probability matrix that overlaps the dynamic evolution process of urban resilience over time with the probability of changes in adjacent periods [54], thereby reflecting the dynamic development characteristics of urban resilience.

In this model, the state transition probability  $P_{ij}$  represents the probability of belonging to the resilience level  $i$  at time  $t$  to belonging to the resilience level  $j$  at time  $t + 1$ . The calculation formula is as follows:

$$P_{ij} = \frac{n_{ij}}{n_i} \tag{32}$$

In the above formula,  $n_{ij}$  represents the total number of cities that have transitioned from the resilience level  $i$  at time  $t$  to  $j$  at time  $t + 1$ ; and  $n_i$  represents the total number of cities belonging to resilience level  $i$  in all years of transfer. Furthermore, based on the resilience is divided into five levels, corresponding to a  $5 \times 5$  state transition probability matrix [55], as shown in Table 5, where  $0 \leq P_{ij} \leq 1$  and  $\sum_{j=1}^5 P_{ij} = 1$  [56].

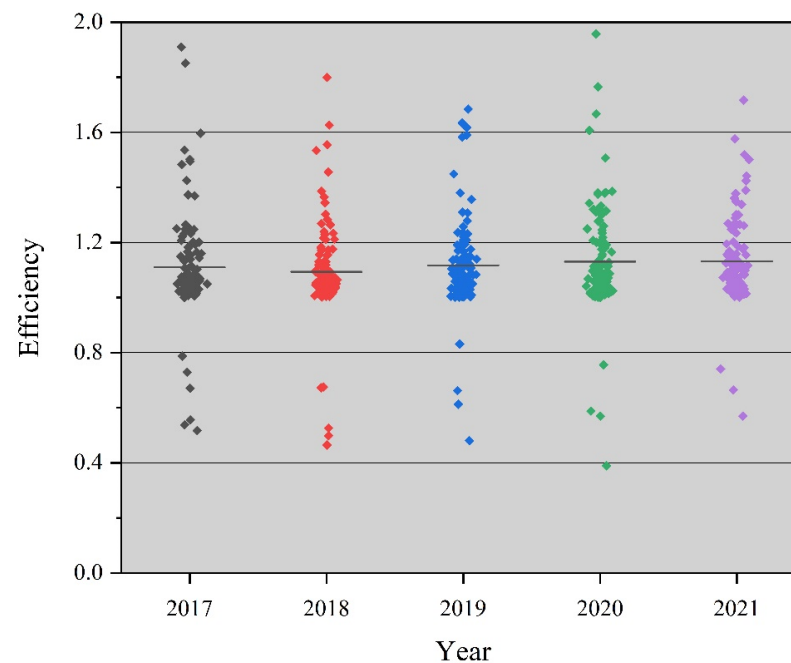
**Table 5.** State transition probability matrix.

$t \setminus t + 1$	Low	Medium-Low	Medium	Medium-High	High
Low	$P_{11}$	$P_{12}$	$P_{13}$	$P_{14}$	$P_{15}$
Medium-Low	$P_{21}$	$P_{22}$	$P_{23}$	$P_{24}$	$P_{25}$
Medium	$P_{31}$	$P_{32}$	$P_{33}$	$P_{34}$	$P_{35}$
Medium-High	$P_{41}$	$P_{42}$	$P_{43}$	$P_{44}$	$P_{45}$
High	$P_{51}$	$P_{52}$	$P_{53}$	$P_{54}$	$P_{55}$

### 3. Case Study

#### 3.1. Calculation Results of the Urban Resilience Level

Based on the Super-SBM model described in Section 2.2, the resilience efficiency of 105 large Chinese cities from 2017 to 2021 was calculated using the software MaxDEA (v12.1). Figure 6 shows their scatter plot distribution. It can be seen that target cities' resilience efficiency is concentrated in the (1,1.2) range, and fewer cities have high or low resilience.

**Figure 6.** Scatter plot of resilience efficiency values in 105 large cities from 2017 to 2021.

In order to more intuitively present the development of resilience during the research period, as well as the difference between cities, ArcGIS was used to visualize the resilience levels of each year. According to the natural fracture point method, 105 cities are divided into five levels, and their distribution is obtained as shown in Figure 7.

Figure 7 shows a significant difference in the number of cities with different resilience levels. The overall distribution of resilience follows an olive-shaped structure, with most cities having moderate resilience. The number of cities with medium-high and medium-low resilience is similar. In contrast, the number of cities at the top and bottom is relatively small, resulting in a relatively healthy distribution structure. Specifically, no city's resilience consistently decreased during the research period. Qiqihar, Nanjing, Taizhou, Yueyang, and Xining have consistently improved resilience, indicating that they have made tremendous progress in their past socio-economic development and urban transformation. With time, they may achieve further balanced development of various elements of urban resilience in the future [48]. Among the other cities, the resilience of most cities, such as Xiangyang and Guangzhou, has not changed much; they are basically in a continuous fluctuation state with no significant improvement in resilience.

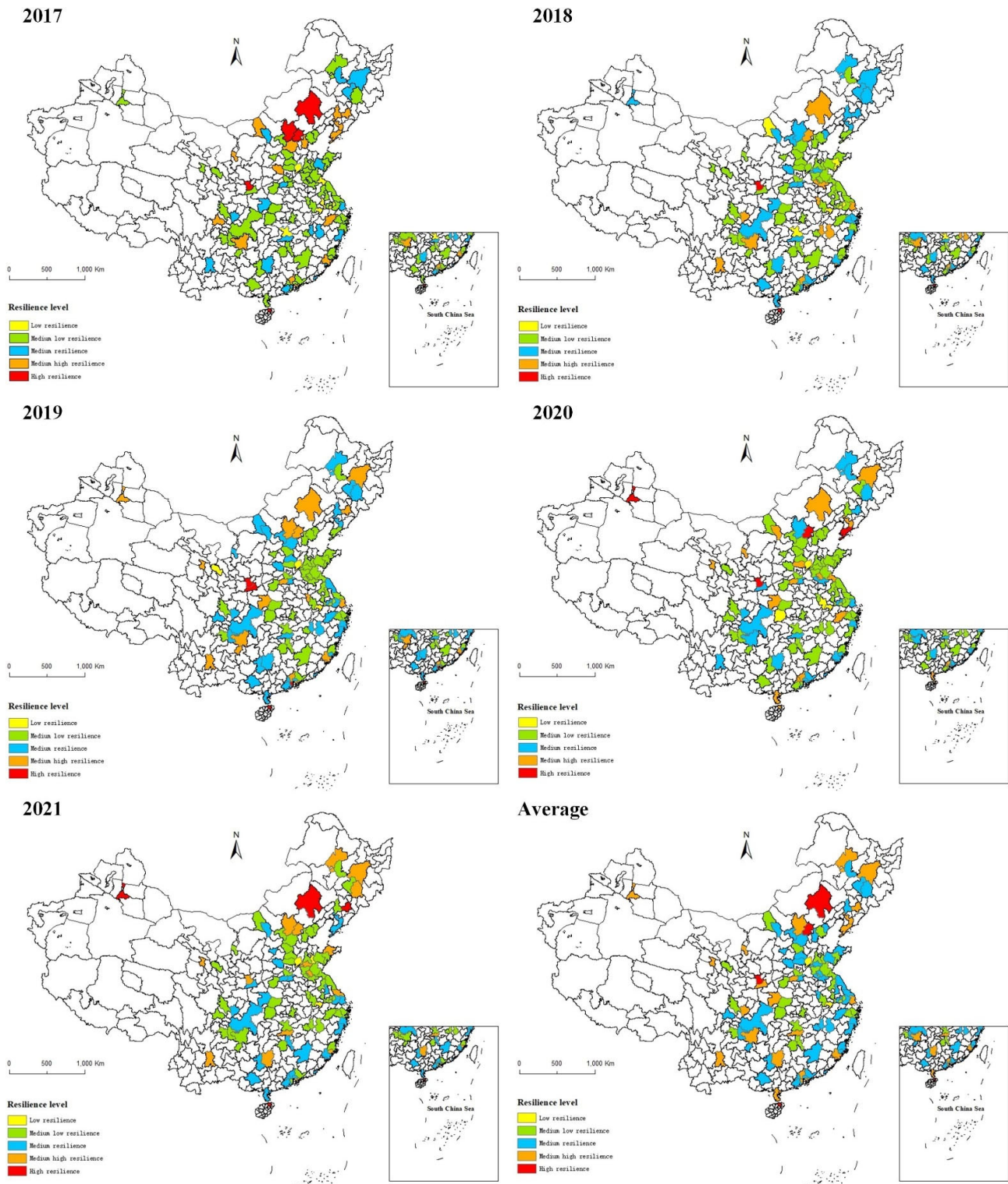


**Figure 7.** Resilience level distribution from 2017 to 2021.

According to the calculation results, Figure 8 shows the efficiency changes of the top and bottom five cities in terms of comprehensive resilience level from 2017 to 2021. The top five cities are Haikou, Xianyang, Jinjiang, Cixi, and Kunshan. In comparison, the bottom five cities are Liaocheng, Wuhu, Yueyang, Wuxi, and Yichang. Only Haikou has a higher administrative level and great resilience.

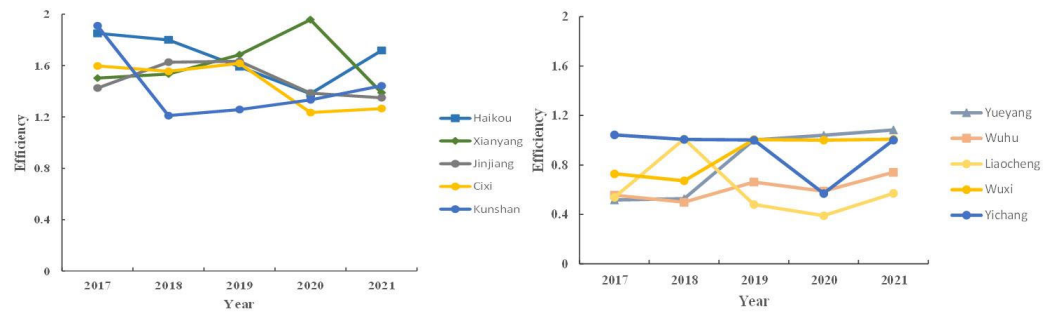


Figure 8. Top and bottom five cities with resilience from 2017 to 2021.

Liaocheng and Wuhu are the two cities with the lowest resilience, with an average efficiency of only 0.598 and 0.609, respectively. There is a large gap between them and other cities. They are located in eastern China, with a relatively developed economy and proximity to provincial capitals or central cities. Their lower resilience may be due to the lack of coordinated development between various aspects, including economy, society, and environment, or may be influenced by the siphoning effect of neighboring central cities [56], which disrupt urban development and make positioning problematic. Tail cities' resilience changes are more stable than the top cities, and the trend tends to be consistent. This indicates that they currently lack the motivation to improve resilience significantly.

### 3.2. Calculation Results of the Dynamic Level

Based on Formulas (11) to (17), the dynamic evolution of comprehensive resilience and the Malmquist decomposition index in each city was calculated. The average Malmquist decomposition index of all cities in each year is shown in Table 6, and the dynamic evolution is shown in Figure 9.

Table 6. Decomposition of the Malmquist index during the research period.

Period	EFFCH	TECH	TFPCH
2017–2018	0.998	0.982	0.974
2018–2019	1.041	1.020	1.044
2019–2020	1.017	1.200	1.228
2020–2021	1.018	0.909	0.923

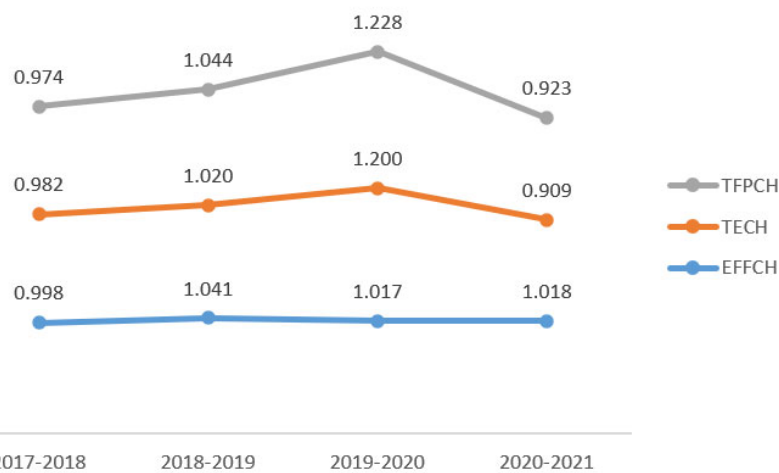


Figure 9. Dynamic evolution of the Malmquist index during the research period.

Table 6 and Figure 9 show that the Malmquist decomposition index remained stable during the study period, showing a trend of first increasing and then decreasing, and the results of each index are distributed around 1. Overall, the average total factor productivity

is 1.042, indicating a slow improvement in comprehensive urban resilience, with an average annual growth rate of 4.2%. The mean values of technological efficiency change and technological change are 1.018 and 1.028, respectively, with an average annual growth rate of 1.8% and 2.8%, respectively. The contribution of technological change is slightly more outstanding than technological efficiency changes. This result indicates that the overall resilience of large Chinese cities shows a healthy situation; their development is full of vitality but not yet mature [46].

From the time series perspective, the Malmquist index in 2017–2018 and 2020–2021 is smaller than 1, while that in 2018–2019 and 2019–2020 is greater than 1. During the period of increasing total factor productivity, the Malmquist index was highest in 2019–2020, with a comprehensive efficiency increase of 22.8%. The decomposed technical efficiency and technical changes are 1.200 and 1.017, respectively, indicating that the resilience improvement in that year mainly depends on changes in technical efficiency. The impact of technical changes is relatively small. In addition, the number of cities with a Malmquist index greater than 1 in each period is 38, 66, 86, and 35, with the highest number in 2019–2020 and the lowest number in 2020–2021, even less than half of the previous year. In cities with a Malmquist index greater than 1 in 2019–2020, the average values of EFFCH and TECH are 1.048 and 1.225, indicating that productivity improvement mainly relies on technological progress. In cities with a Malmquist index greater than 1 in 2020–2021, the average values of EFFCH and TECH are 1.128 and 0.966, indicating a technological decline. However, the contribution of technological efficiency has further increased. Hence, the improvement of productivity mainly depends on technological efficiency. This indicates that in the field of urban resilience, technological progress has a significant impact on total factor productivity. The significant gap between the adjacent 2 years is that the impact of technological progress on urban resilience is gradually decreasing. Compared to improving technological efficiency, the promoting effect of technological progress on urban resilience is more prominent.

### 3.3. Calculation Results of the Spatial Equilibrium

In order to further analyze the regional difference in the resilience of 105 large cities, this study uses the principle of the Dagum Gini coefficient and Formulas (18) to (31). This study groups 105 large cities into eastern, central, and western regions. The Gini coefficient of large cities' resilience from 2017 to 2021 was calculated and decomposed, and the results are shown in Table 7.

**Table 7.** The Dagum Gini coefficient and its decomposition results.

Year	G	Intra-Regional Difference			Inter-Regional Difference			Contribution Rates		
		East	Middle	West	East	Middle	West	East	Middle	West
2017	0.085	0.097	0.076	0.053	0.089	0.077	0.066	43.807	12.853	43.340
2018	0.077	0.074	0.088	0.059	0.084	0.068	0.077	40.713	20.555	38.732
2019	0.074	0.073	0.055	0.091	0.066	0.086	0.081	39.755	18.366	41.879
2020	0.086	0.080	0.085	0.096	0.085	0.090	0.096	39.249	22.343	38.408
2021	0.071	0.078	0.057	0.065	0.069	0.072	0.063	42.573	9.667	47.760

Table 7 shows that the overall Dagum Gini coefficient of large cities' resilience fluctuates between 0.071 and 0.086, showing an overall downward trend during the research period. From 2017 to 2019, the overall Gini coefficient continued to decline, from 0.085 to 0.074, with an average annual decrease of 6.69%. Nevertheless, in 2020, it suddenly rebounded, reaching a peak of 0.086, slightly higher than in 2017. Subsequently, it continues to decline in 2021, reaching a minimum value of 0.071, lower than the level in 2019, with a decrease of 17.44%. Overall, the decline process is not stable, and there is a tendency for rebounds to occur with a large amplitude. However, it still maintains an overall down-

ward trend. During this process, the regional difference in the resilience of Chinese cities gradually narrowed [8].

Figure 10 further illustrates the contribution of each decomposition coefficient and the evolution of their contribution rates. From the perspective of contribution, there are varying degrees of changes in each part's contribution during the research period, but the overall contribution rate remains stable, and its changes are mainly concentrated in  $G_{nb}$ . Although the continuous fluctuation of contribution changes is more pronounced, the contribution and proportion of  $G_{nb}$  have always been low, less than 20% for many years. The contribution rates of  $G_w$  and  $G_t$  are similar, reaching around 40%, indicating that the spatial difference in large cities' resilience mainly comes from differences within subregions and super-density. The impact of the difference between subregions is relatively tiny.

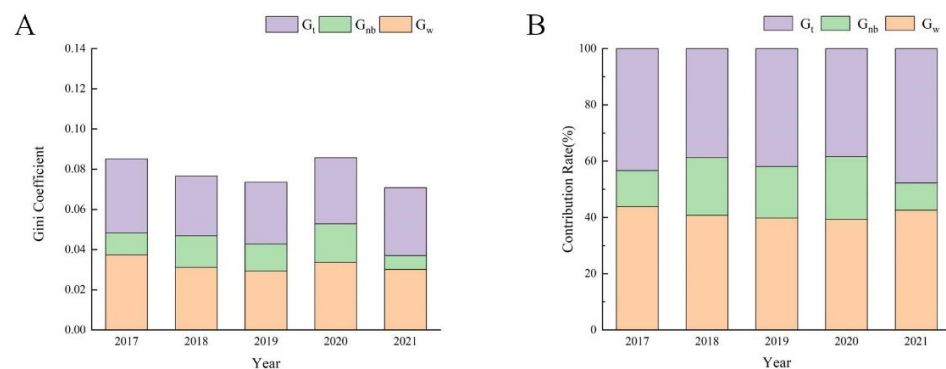


**Figure 10.** The results of the Dagum Gini coefficient and its decomposition. (A) The contribution value of  $G_w$ ,  $G_t$  and  $G_{nb}$  from 2017 to 2021. (B) The contribution rate of  $G_w$ ,  $G_t$  and  $G_{nb}$  from 2017 to 2021.

The analysis of the evolution process shows that  $G_w$  has generally decreased from 0.037 in 2017 to 0.030 in 2021, but there is a certain degree of rebound in 2020;  $G_{nb}$  fluctuated repeatedly and has a large amplitude and its maximum and minimum contributions occurred in 2020 and 2021, with a contribution rate of only 9.67% in 2021; and  $G_t$  underwent a process of first decreasing and then continuously increasing, showing a U-shaped development trend. Its contribution in 2021 is close to that in 2017. In addition, the change of  $G_w$  shows a downward trend, and the contribution of difference within subregions to the overall difference gradually decreases. Since 2019, it has been smaller than super variable density, but their contributions are still relatively close.

Figure 11A reflects the difference and its evolution within the three subregions. The average Gini coefficient in the eastern, central, and western subregions is 0.080, 0.072, and 0.073. The highest is found in the eastern subregion, and the central subregion is slightly lower than the western subregion, indicating a significant difference within large cities in eastern China. The development trajectory of the eastern region is similar to the overall Gini coefficient, showing a slow downward trend, with an average annual decrease of 4.90%. The overall stability indicates that the internal difference between large cities in eastern China is decreasing yearly. However, that internal difference is still significant due to the large base and weak decline. The Gini coefficient in the central and western regions varies significantly and exhibits completely different changes. Only the western region has a higher difference in 2021 than in 2017, maintaining a significant annual growth rate of 27.04% from 2017 to 2020. During this period, the difference in urban resilience continued to increase rapidly, followed by a sudden and significant decrease of over 30% in 2021. However, the Gini coefficient remained higher than in 2017, and the regional difference increased. Although the central region has the slightest internal difference, its development shows excellent instability. It remains a fluctuating state with no sustained growth or decline during the research period.

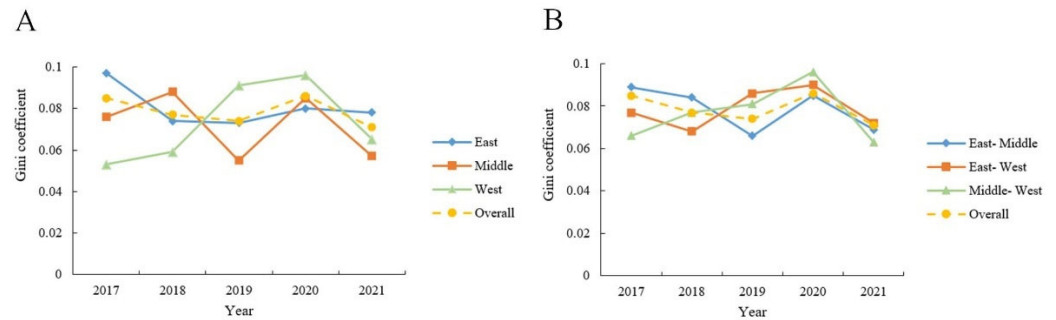


**Figure 11.** The results of the Dagum Gini coefficient and its decomposition. (A) The Gini coefficient of subregions in large cities from 2017 to 2021. (B) The extended Gini coefficient between subregions in large cities from 2017 to 2021.

Based on the results, there is indeed a significant polarization phenomenon in the eastern region. Haikou, Jinjiang, Cixi, and other cities with high-efficiency rankings and Liaocheng, Wuhu, and other cities with low-efficiency rankings all belong to the eastern cities, and the difference is significantly higher than that in the central and western regions. However, central and western regions are both limited by economic and social conditions, and there is greater uncertainty in their development. Except for the provincial capital, the resilience development level of other cities is relatively concentrated. Hence, the difference between cities is relatively small [57].

From the perspective of difference between subregions, Figure 11B describes the subregional difference and evolution of resilience in large cities. The distribution curve of the difference level between each subregion is relatively close, located in the same interval. The average difference between the eastern-central subregion and the eastern-western subregion is the same, all of which is 0.079. The difference between the central-western subregion is slightly smaller, with an average of 0.077, so the difference between subregions can be ignored. At the same time, it can also be seen that the subregional difference in urban resilience showed an unstable trend with no complete upward or downward process. Only the difference between central-western continued to widen from 0.066 to 0.096 in 2017–2020. Compared to 2017, the difference between each subregion decreased in 2021, with the most significant decrease being in the eastern-central region, reaching 22.47%. The difference between eastern and central regions has decreased by 6.49% and 4.55%, indicating that the difference between subregions is gradually narrowing, and the development of resilience is showing a unified trend. From the perspective of evolution, the difference between eastern-central and eastern-western regions shows a similar development trajectory. In the early stage of the research phase, it gradually decreases. Then, after a brief increase, it decreases again, all with little change. The difference between the central and western regions maintains an average annual growth rate of 31.25% in the first 4 years. Then, it drops to the minimum value of 0.063 in 2021.

### 3.4. Calculation Results of the Dynamic Evolution

Based on the definition of the Markov chain and Formula (32), the probability matrix of resilience state transition for 105 large cities was obtained, as shown in Table 8:

**Table 8.** Probability matrix of resilience state transition in 105 large cities in China.

$t \setminus t+1$	Low	Medium-Low	Medium	Medium-High	High
Low	0.622222	0.211111	0.111111	0.033333	0.022222
Medium-Low	0.188235	0.376471	0.247059	0.117647	0.070588
Medium	0.084337	0.192771	0.39759	0.228916	0.096386
Medium-High	0	0.111111	0.185185	0.407407	0.296296
High	0.049383	0.049383	0.08642	0.246914	0.567901

Table 7 shows three findings. (1) The resilience of large Chinese cities is dependent on a strong path. The probability values on the diagonal in the matrix are significantly higher than those on the non-diagonal, indicating that urban resilience tends to remain stable and has good stability [58]. Among them, the probability of maintaining the same level for each resilience level is 62.22%, 37.65%, 39.76%, 40.74%, and 56.79%. This indicates that cities with low resilience have the highest probability of maintaining the same level, reaching 62.22% among large cities. In contrast, cities with medium-low resilience have the lowest probability of maintaining the same level, at 37.65%. In non-diagonal probability values, the maximum value is 0.296, indicating that the maximum probability of urban resilience level transfer is only 29.63%. At the same time, the probability of high and low resilience at both ends of the diagonal is higher. The lower probability in the middle indicates that transfer is more likely to occur when the resilience level is moderate. It is easier to maintain stability when the resilience level approaches the two poles. (2) The probability value close to the diagonal is higher than the probability values on non-diagonal lines. This indicates that if the urban resilience level shifts, it tends toward adjacent resilience levels, making it more challenging to cross levels. Taking medium-high resilience as an example, the probability of transitioning to medium and high resilience is 18.52% and 29.63%. In comparison, the probability of transitioning to medium resilience is only 11.11%, and the probability of transitioning to low resilience is 0. The analysis of the reasons for this suggests that resilience construction is a long-term and continuous investment process. A city's resilience makes it difficult to undergo significant changes quickly, making it challenging to transfer resilience across multiple levels. (3) The probability value on the right side of the diagonal is generally greater than that on the left side, indicating that the probability of resilience level shifting to higher levels is higher than that toward lower levels. Resilience tends to improve toward higher levels. For example, the probability of an increase from medium-low to medium resilience is 24.71%. The probability of a decrease from medium-low to low resilience is 18.82%. However, the level of difference is not significant. Transferring to a higher level does not have many advantages, and this advantage may be eliminated at any time. For example, the probabilities of medium and medium-high resilience shifting upwards and downwards are 22.89% and 19.28%, 29.63% and 18.52%; the minimum difference is only about 3%, and the maximum difference is not more than 15%. Therefore, it can only indicate that the overall resilience development of large cities shows a healthy situation, but the current state is unstable.

#### 4. Discussion

The evaluation results demonstrate that 105 large cities have achieved good results in resilience construction, with most cities achieving DEA effectiveness and maintaining a specific growth rate. However, resilience's slow improvement still needs to be taken seriously. Although resilience goals have been frequently mentioned in the planning of various cities, there is still a lack of specific measures for urban transformation, ecological environment protection, and industrial structure upgrading [7]. Therefore, it is recommended that the government and stakeholders participate in the construction together and carry out the resilience improvement in a planned manner. In addition, the government must fully recognize the balance between the driving force, pressure, state, impact, and response subsystems [24], strengthen restrictions on pressure, focus on ecological improvement and social security, analyze the demand for resilience, and improve resource investment structures.

Based on the results of the Super-SBM model, the top ten cities with the highest and lowest average resilience were identified, as shown in Figure 12. The top ten cities with the highest resilience mainly belong to coastal provinces, including cities of various sizes, such as Kunshan and Shenzhen. Although their strengths differ significantly, the eastern coastal regions are conducive to their socio-economy and resilience development. Beijing's high resilience has been confirmed by other studies [59]. Urumqi is vast and sparsely populated, and its urban development is influenced by the Western Development Strategy, which benefits its resilience construction [60]. While among the ten cities with the lowest

resilience, specific differences exist in their sizes and types. For example, Nanjing and Lanzhou are provincial capital cities in the eastern and western regions. Although there is a significant difference in their urban size, their resilience is similarly low. Central cities such as Nanjing and Qingdao have a high degree of social modernization. However, their urban development and resilience construction may be somewhat disconnected, and population pressure hinders the improvement of urban resilience. Small and medium-sized cities such as Zibo and Yichang may face many problems, such as an aging population, lagging economic structure, and ecological environment damage, which limit their resilience.

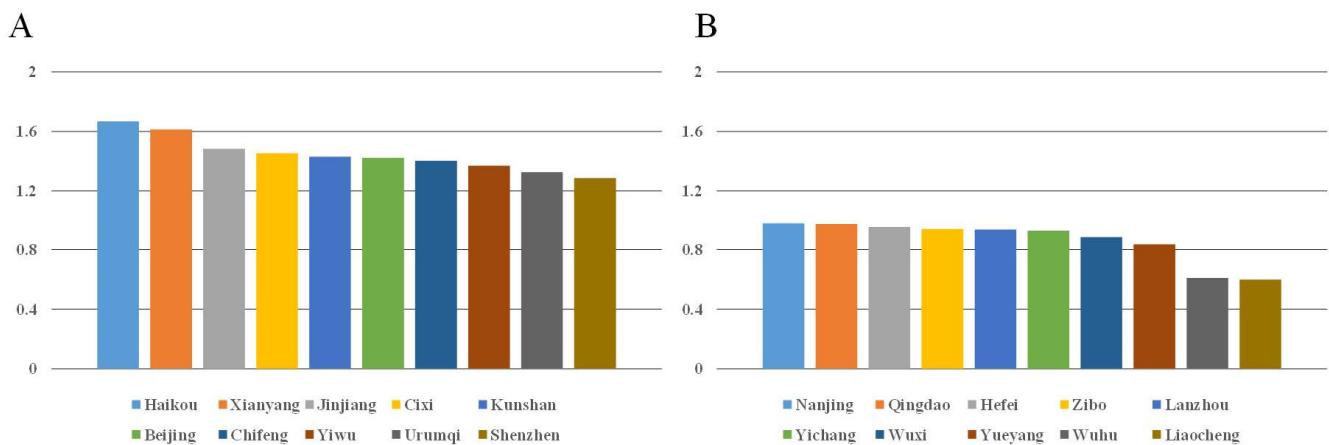


**Figure 12.** Top and bottom ten cities in terms of average resilience. (A) Ten cities with the highest average resilience. (B) Ten cities with the lowest average resilience.

The combined effect of technological efficiency improvement and technological progress results in resilience gradually improving, but the process is slow. From the perspective of the decomposition index, there is not much difference in the contribution between technological progress and technological efficiency improvement, so more attention should be paid to improving management planning. To maximize the potential of existing technologies and improve resource utilization, each city could start by improving its management, updating technology, etc. Secondly, in the face of natural disasters, cities urgently need scientific disaster prevention and reduction plans. Community leaders should strive to popularize emergency self-rescue methods to the public and cultivate residents' awareness of emergency safety. In addition, emergency infrastructure should be improved, and emergency material supply channels that can respond quickly should be established.

The current narrowing of differences in resilience is a positive signal that the distribution is gradually becoming more balanced. However, the internal differences among subregions still deserve attention, with the eastern subregion having the greatest. As the most developed region in China, there are significant differences in each eastern city. The central city has a large concentration of transportation, education, and medical resources, with a higher social modernization and advantages in resilience construction. Surrounding cities are easily affected by siphons, and issues such as population outflow and environmental pollution are all worth paying attention to. Therefore, from the perspective of urban planners, it is necessary to properly clarify the positioning of cities, strengthen interconnections, and do an excellent job at the top-level design of urban layout within the region. The central city continues strengthening scientific innovation, optimizing the social security system, and increasing environmental protection efforts. Surrounding cities actively improve infrastructure, attract talents to settle in, and do a good job supporting the central city.

The results of the Markov chain show that the resilience of large Chinese cities will exhibit good stability in the future, with a small probability of a decrease but also a low probability of an improvement. Larger cities occupy more resources but bear more significant population pressure. Their infrastructure is overwhelmed due to the inability

to match population demand. Smaller cities experience population loss, which could make the infrastructure inadequate and outdated. Therefore, it is necessary to strengthen infrastructure in the current stage of resilience construction. Firstly, cities should strengthen public transportation and improve the urban transportation environment [61]. Convenient transportation is the fundamental guarantee for strengthening urban connections and enhancing commercial exchanges. Secondly, the infrastructure related to social security, including education, healthcare, and other areas related to people's livelihoods, should be improved. Finally, the ecological sector remains a crucial focus of urban resilience. Measures such as improving greening, increasing urban wetland areas, strictly controlling pollution, and strengthening atmospheric governance should continue to be taken.

Based on the previous analysis and discussion, it is fully demonstrated that the evaluation model of this study is feasible. This study accurately obtained the resilience distribution pattern of 105 large Chinese cities. At the same time, the resilience mechanism is deeply explored, the process of enhancing resilience is analyzed, and targeted suggestions are proposed based on the results, which other methods do not possess.

## 5. Conclusions

Accurately assessing resilience and its evolution is significant for enhancing the stability of current large cities. This study proposed a novel urban resilience assessment model, established an evaluation indicator system based on the DPSIR-DEA model, and conducted a case study on 105 large Chinese cities. The results indicate that this assessment model is objective and practical. The DPSIR model can accurately depict complex behaviors of urban resilience and construct complete logical relationships for it. The DEA model is equally compatible with urban resilience evaluation. It provides an accurate and efficient way to measure urban resilience.

This study measured the resilience of 105 large Chinese cities from 2017 to 2021. It analyzed their dynamic evolution characteristics and regional differences. Three conclusions can be drawn. Firstly, their overall resilience is relatively high, with a healthy olive-shaped distribution structure, but there is a significant polarization phenomenon. Secondly, from the perspective of dynamic evolution, comprehensive resilience has experienced a development trend that first increased and then decreased during the research period. The overall efficiency improvement depends on the combined effect of technological efficiency improvement and technological progress. In future predictions, the resilience will have good stability, and there is a certain probability that it will continue to improve. Finally, the regional difference of 105 large cities' resilience is gradually narrowing. Currently, the internal difference in the eastern subregion is the largest, while the difference between the central and western subregions is the smallest.

Due to factors including perspective selection and data limitations, only relatively important and representative indicators were selected, and the research period was only set from 2017 to 2021. The latest evaluation results could not be obtained temporarily; therefore, the results may not be comprehensive. This is a limitation of this study, and it will be the focus of the author's further research. In the future, when establishing an evaluation index system, the author will comprehensively consider the characteristics and elements of urban resilience and thoroughly consider urban behavior under the influence of risks. Future research will further expand the sample range, time, and city matrix to establish a more comprehensive and complete urban resilience assessment model. Our research team will conduct a comparative analysis with cities from other countries or regions by collecting more research data.

**Author Contributions:** L.J. and B.H. designed the research, conducted part of the analysis and wrote the paper. Q.T., Y.Z., X.H., L.W. and Y.W. collected data and conducted part of the analysis. All authors have read and agreed to the published version of the manuscript.

**Funding:** This research was funded by the National Social Science Foundation of China (No. 23XJY018), the Chongqing Education Commission Humanities and Social Science Research Project (No. 23SKGH137), the National Natural Science Foundation of China (Grant No. 71901043, No. 72004187 and No. 72204033), the Natural Science Foundation of Chongqing (Grant No. CSTB2022NSCQ-MSX0390) and the Chongqing Graduate Research Innovation Project (No. CYS240506).

**Data Availability Statement:** The raw data supporting the conclusions of this article will be made available by the authors on request.

**Conflicts of Interest:** The authors declare no competing interests.

## References

- Zhang, J.; Yang, X.; Lu, D. Evaluation of Urban Resilience Based on Trio Spaces: An Empirical Study in Northeast China. *Buildings* **2023**, *13*, 1695. [[CrossRef](#)]
- Xu, W.; Cong, J.; Proverbs, D.; Zhang, L. An Evaluation of Urban Resilience to Flooding. *Water* **2021**, *13*, 2022. [[CrossRef](#)]
- Chen, Y.; Zhu, M.; Zhou, Q.; Qiao, Y. Research on Spatiotemporal Differentiation and Influence Mechanism of Urban Resilience in China Based on MGWR Model. *Int. J. Environ. Res. Public Health* **2021**, *18*, 1056. [[CrossRef](#)] [[PubMed](#)]
- Zhong, Q.; Chen, Y.; Yan, J. Comprehensive Evaluation of Community Human Settlement Resilience and Spatial Characteristics Based on the Supply–Demand Mismatch between Health Activities and Environment: A Case Study of Downtown Shanghai, China. *Glob. Health* **2023**, *19*, 87. [[CrossRef](#)] [[PubMed](#)]
- Meerow, S.; Pajouhesh, P.; Miller, T.R. Social Equity in Urban Resilience Planning. *Local Environ.* **2019**, *24*, 793–808. [[CrossRef](#)]
- Gavari-Starkie, E.; Casado-Claro, M.-F.; Navarro-González, I. The Japanese Educational System as an International Model for Urban Resilience. *Int. J. Environ. Res. Public Health* **2021**, *18*, 5794. [[CrossRef](#)] [[PubMed](#)]
- Shao, Y.; Sun, Y.; Zheng, Z. How Do Comprehensive Territorial Plans Frame Resilience? A Content Analysis of Plans by Major Cities in China. *Sustainability* **2023**, *15*, 7783. [[CrossRef](#)]
- Liu, X.; Li, S.; Xu, X.; Luo, J. Integrated Natural Disasters Urban Resilience Evaluation: The Case of China. *Nat. Hazards* **2021**, *107*, 2105–2122. [[CrossRef](#)]
- Liu, Y.; Li, Q.; Li, W.; Zhang, Y.; Pei, X. Progress in Urban Resilience Research and Hotspot Analysis: A Global Scientometric Visualization Analysis Using CiteSpace. *Environ. Sci. Pollut. Res.* **2022**, *29*, 63674–63691. [[CrossRef](#)]
- Meerow, S.; Stults, M. Comparing Conceptualizations of Urban Climate Resilience in Theory and Practice. *Sustainability* **2016**, *8*, 701. [[CrossRef](#)]
- Zhang, X.; Mao, F.; Gong, Z.; Hannah, D.M.; Cai, Y.; Wu, J. A Disaster-Damage-Based Framework for Assessing Urban Resilience to Intense Rainfall-Induced Flooding. *Urban Clim.* **2023**, *48*, 101402. [[CrossRef](#)]
- Vargas-Hernández, J.G.; Zdunek-Wielgołaska, J. Urban Green Infrastructure as a Tool for Controlling the Resilience of Urban Sprawl. *Environ. Dev. Sustain.* **2021**, *23*, 1335–1354. [[CrossRef](#)]
- Zhang, Z.; Zhang, J.; Zhang, Y.; Chen, Y.; Yan, J. Urban Flood Resilience Evaluation Based on GIS and Multi-Source Data: A Case Study of Changchun City. *Remote Sens.* **2023**, *15*, 1872. [[CrossRef](#)]
- Xun, X.; Yuan, Y. Research on the Urban Resilience Evaluation with Hybrid Multiple Attribute TOPSIS Method: An Example in China. *Nat. Hazards* **2020**, *103*, 557–577. [[CrossRef](#)] [[PubMed](#)]
- Qiao, H.; Pei, J. Urban Stormwater Resilience Assessment Method Based on Cloud Model and TOPSIS. *Int. J. Environ. Res. Public Health* **2021**, *19*, 38. [[CrossRef](#)]
- Zhang, Y.; Yue, W.; Su, M.; Teng, Y.; Huang, Q.; Lu, W.; Rong, Q.; Xu, C. Assessment of Urban Flood Resilience Based on a Systematic Framework. *Ecol. Indic.* **2023**, *150*, 110230. [[CrossRef](#)]
- Ji, J.; Chen, J. Urban Flood Resilience Assessment Using RAGA-PP and KL-TOPSIS Model Based on PSR Framework: A Case Study of Jiangsu Province, China. *Water Sci. Technol.* **2022**, *86*, 3264–3280. [[CrossRef](#)] [[PubMed](#)]
- Zhang, M.; Chen, W.; Cai, K.; Gao, X.; Zhang, X.; Liu, J.; Wang, Z.; Li, D. Analysis of the Spatial Distribution Characteristics of Urban Resilience and Its Influencing Factors: A Case Study of 56 Cities in China. *Int. J. Environ. Res. Public Health* **2019**, *16*, 4442. [[CrossRef](#)] [[PubMed](#)]
- Moghadas, M.; Asadzadeh, A.; Vafeidis, A.; Fekete, A.; Kötter, T. A Multi-Criteria Approach for Assessing Urban Flood Resilience in Tehran, Iran. *Int. J. Disaster Risk Reduct.* **2019**, *35*, 101069. [[CrossRef](#)]
- Zhou, R.; Yu, Y.; Wu, B.; Luo, X. Quantitative Evaluation of Urban Resilience in Underdeveloped Regions: A Study of Six Cities in Sichuan & Tibet, China. *Front. Environ. Sci.* **2023**, *11*, 1133595. [[CrossRef](#)]
- Zhang, H.; Liu, X.; Xie, Y.; Gou, Q.; Li, R.; Qiu, Y.; Hu, Y.; Huang, B. Assessment and Improvement of Urban Resilience to Flooding at a Subdistrict Level Using Multi-Source Geospatial Data: Jakarta as a Case Study. *Remote Sens.* **2022**, *14*, 2010. [[CrossRef](#)]
- Tayyab, M.; Zhang, J.; Hussain, M.; Ullah, S.; Liu, X.; Khan, S.N.; Baig, M.A.; Hassan, W.; Al-Shaibah, B. GIS-Based Urban Flood Resilience Assessment Using Urban Flood Resilience Model: A Case Study of Peshawar City, Khyber Pakhtunkhwa, Pakistan. *Remote Sens.* **2021**, *13*, 1864. [[CrossRef](#)]
- Xu, H.; Li, Y.; Wang, L. Resilience Assessment of Complex Urban Public Spaces. *Int. J. Environ. Res. Public Health* **2020**, *17*, 524. [[CrossRef](#)] [[PubMed](#)]

24. Yang, G.; Gui, Q.; Liu, J.; Chen, X.; Cheng, S. Spatial-Temporal Evolution and Driving Factors of Ecological Security in China Based on DPSIR-DEA Model: A Case Study of the Three Gorges Reservoir Area. *Ecol. Indic.* **2023**, *154*, 110777. [[CrossRef](#)]
25. Ling, T.-Y. Investigating the Malleable Socioeconomic Resilience Pathway to Urban Cohesion: A Case of Taipei Metropolitan Area. *Environ. Dev. Sustain.* **2021**, *23*, 13016–13041. [[CrossRef](#)]
26. Hu, Q.; He, X. An Integrated Approach to Evaluate Urban Adaptive Capacity to Climate Change. *Sustainability* **2018**, *10*, 1272. [[CrossRef](#)]
27. Li, H.; Lin, Y.; Wang, Y.; Liu, J.; Liang, S.; Guo, S.; Qiang, T. Multi-Criteria Analysis of a People-Oriented Urban Pedestrian Road System Using an Integrated Fuzzy AHP and DEA Approach: A Case Study in Harbin, China. *Symmetry* **2021**, *13*, 2214. [[CrossRef](#)]
28. Li, X.; Zhan, J.; Lv, T.; Wang, S.; Pan, F. Comprehensive Evaluation Model of the Urban Low-Carbon Passenger Transportation Structure Based on DPSIR. *Ecol. Indic.* **2023**, *146*, 109849. [[CrossRef](#)]
29. Chen, J.; Li, Q.; Wang, H.; Deng, M. A Machine Learning Ensemble Approach Based on Random Forest and Radial Basis Function Neural Network for Risk Evaluation of Regional Flood Disaster: A Case Study of the Yangtze River Delta, China. *Int. J. Environ. Res. Public Health* **2019**, *17*, 49. [[CrossRef](#)]
30. Wang, S.; Sun, C.; Li, X.; Zou, W. Sustainable Development in China's Coastal Area: Based on the Driver-Pressure-State-Welfare-Response Framework and the Data Envelopment Analysis Model. *Sustainability* **2016**, *8*, 958. [[CrossRef](#)]
31. Li, Z.; Wei, Y.; Li, Y.; Wang, Z.; Zhang, J. China's Provincial Eco-Efficiency and Its Driving Factors—Based on Network DEA and PLS-SEM Method. *Int. J. Environ. Res. Public Health* **2020**, *17*, 8702. [[CrossRef](#)] [[PubMed](#)]
32. Jiao, L.; Wang, L.; Lu, H.; Fan, Y.; Zhang, Y.; Wu, Y. An Assessment Model for Urban Resilience Based on the Pressure-State-Response Framework and BP-GA Neural Network. *Urban Clim.* **2023**, *49*, 101543. [[CrossRef](#)]
33. Hammond, M.; Chen, A.S.; Batica, J.; Butler, D.; Djordjević, S.; Gourbesville, P.; Manojlović, N.; Mark, O.; Veerbeek, W. A New Flood Risk Assessment Framework for Evaluating the Effectiveness of Policies to Improve Urban Flood Resilience. *Urban Water J.* **2018**, *15*, 427–436. [[CrossRef](#)]
34. Kazuva, E.; Zhang, J.; Tong, Z.; Si, A.; Na, L. The DPSIR Model for Environmental Risk Assessment of Municipal Solid Waste in Dar Es Salaam City, Tanzania. *Int. J. Environ. Res. Public Health* **2018**, *15*, 1692. [[CrossRef](#)]
35. Sarkki, S.; Ficko, A.; Wielgolaski, F.; Abraham, E.; Bratanova-Doncheva, S.; Grunewald, K.; Hofgaard, A.; Holtmeier, F.; Kyriazopoulos, A.; Broll, G.; et al. Assessing the Resilient Provision of Ecosystem Services by Social-Ecological Systems: Introduction and Theory. *Clim. Res.* **2017**, *73*, 7–15. [[CrossRef](#)]
36. Chen, J.; Ma, H.; Yang, S.; Zhou, Z.; Huang, J.; Chen, L. Assessment of Urban Resilience and Detection of Impact Factors Based on Spatial Autocorrelation Analysis and GeoDetector Model: A Case of Hunan Province. *ISPRS Int. J. Geo-Inf.* **2023**, *12*, 391. [[CrossRef](#)]
37. Suárez, M.; Gómez-Baggethun, E.; Benayas, J.; Tilbury, D. Towards an Urban Resilience Index: A Case Study in 50 Spanish Cities. *Sustainability* **2016**, *8*, 774. [[CrossRef](#)]
38. Zheng, Y.; Xie, X.-L.; Lin, C.-Z.; Wang, M.; He, X.-J. Development as Adaptation: Framing and Measuring Urban Resilience in Beijing. *Adv. Clim. Chang. Res.* **2018**, *9*, 234–242. [[CrossRef](#)]
39. Li, X.; Liu, Y.; Zhang, W.; Wang, Y. Research on an Evaluation Model of Urban Seismic Resilience Based on System Dynamics: A Case Study of Chengdu, China. *Sustainability* **2023**, *15*, 10112. [[CrossRef](#)]
40. Jiao, L.; Wu, F.; Luo, F.; Zhang, Y.; Huo, X. Energy and Environmental Efficiency Evaluation of Transportation Systems in China's 255 Cities. *Front. Environ. Sci.* **2022**, *10*, 950562. [[CrossRef](#)]
41. Zhang, Y.; Mao, Y.; Jiao, L.; Shuai, C.; Zhang, H. Eco-Efficiency, Eco-Technology Innovation and Eco-Well-Being Performance to Improve Global Sustainable Development. *Environ. Impact Assess. Rev.* **2021**, *89*, 106580. [[CrossRef](#)]
42. Li, G.; Zhou, Y.; Liu, F.; Wang, T. Regional Differences of Manufacturing Green Development Efficiency Considering Undesirable Outputs in the Yangtze River Economic Belt Based on Super-SBM and WSR System Methodology. *Front. Environ. Sci.* **2021**, *8*, 631911. [[CrossRef](#)]
43. Tang, X.; Zhang, Q.; Li, C.; Zhang, H.; Xu, H. The Effects and Driving Factors of Low-Carbon Transition of International Oil Companies: Evidence from a Super-SBM Model. *Energies* **2023**, *17*, 157. [[CrossRef](#)]
44. Zheng, Z. Energy Efficiency Evaluation Model Based on DEA-SBM-Malmquist Index. *Energy Rep.* **2021**, *7*, 397–409. [[CrossRef](#)]
45. Yang, J.; Tang, L.; Mi, Z.; Liu, S.; Li, L.; Zheng, J. Carbon Emissions Performance in Logistics at the City Level. *J. Clean. Prod.* **2019**, *231*, 1258–1266. [[CrossRef](#)]
46. Yin, J.; Tan, Q. Study on Urban Efficiency Measurement and Spatiotemporal Evolution of Cities in Northwest China Based on the DEA-Malmquist Model. *Sustainability* **2019**, *11*, 434. [[CrossRef](#)]
47. Chen, G.; Yang, Z.; Chen, S. Measurement and Convergence Analysis of Inclusive Green Growth in the Yangtze River Economic Belt Cities. *Sustainability* **2020**, *12*, 2356. [[CrossRef](#)]
48. Lu, Y.-y.; He, Y.; Wang, B.; Ye, S.-s.; Hua, Y.; Ding, L. Efficiency Evaluation of Atmospheric Pollutants Emission in Zhejiang Province China: A DEA-Malmquist Based Approach. *Sustainability* **2019**, *11*, 4544. [[CrossRef](#)]
49. Shi, Z.; Huang, H.; Wu, Y.; Chiu, Y.-H.; Qin, S. Climate Change Impacts on Agricultural Production and Crop Disaster Area in China. *Int. J. Environ. Res. Public Health* **2020**, *17*, 4792. [[CrossRef](#)] [[PubMed](#)]
50. Chen, X.; Xing, L.; Zhou, J.; Wang, K.; Lu, J.; Han, X. Spatial and Temporal Evolution and Driving Factors of County Solid Waste Harmless Disposal Capacity in China. *Front. Environ. Sci.* **2023**, *10*, 1056054. [[CrossRef](#)]
51. Cheng, S.; Yu, Y.; Fan, W.; Zhu, C. Spatio-Temporal Variation and Decomposition Analysis of Livelihood Resilience of Rural Residents in China. *Int. J. Environ. Res. Public Health* **2022**, *19*, 10612. [[CrossRef](#)] [[PubMed](#)]

52. Zhou, R.; Jin, J.; Cui, Y.; Ning, S.; Zhou, L.; Zhang, L.; Wu, C.; Zhou, Y. Spatial Equilibrium Evaluation of Regional Water Resources Carrying Capacity Based on Dynamic Weight Method and Dagum Gini Coefficient. *Front. Earth Sci.* **2022**, *9*, 790349. [[CrossRef](#)]
53. Koko, A.F.; Yue, W.; Abubakar, G.A.; Hamed, R.; Alabsi, A.A.N. Monitoring and Predicting Spatio-Temporal Land Use/Land Cover Changes in Zaria City, Nigeria, through an Integrated Cellular Automata and Markov Chain Model (CA-Markov). *Sustainability* **2020**, *12*, 10452. [[CrossRef](#)]
54. Mansour, S.; Ghoneim, E.; El-Kersh, A.; Said, S.; Abdelnaby, S. Spatiotemporal Monitoring of Urban Sprawl in a Coastal City Using GIS-Based Markov Chain and Artificial Neural Network (ANN). *Remote Sens.* **2023**, *15*, 601. [[CrossRef](#)]
55. Duan, J.; Jiao, F.; Zhang, Q.; Lin, Z. Predicting Urban Medical Services Demand in China: An Improved Grey Markov Chain Model by Taylor Approximation. *Int. J. Environ. Res. Public Health* **2017**, *14*, 883. [[CrossRef](#)] [[PubMed](#)]
56. You, X.; Sun, Y.; Liu, J. Evolution and Analysis of Urban Resilience and Its Influencing Factors: A Case Study of Jiangsu Province, China. *Nat. Hazards* **2022**, *113*, 1751–1782. [[CrossRef](#)] [[PubMed](#)]
57. Hu, C.; Ma, X.; Yang, L.; Chang, X.; Li, Q. Spatial-Temporal Variation and Driving Forces of the Synergy of “Pollution Reduction, Carbon Reduction, Green Expansion and Economic Growth”: Evidence from 243 Cities in China. *Front. Ecol. Evol.* **2023**, *11*, 1202898. [[CrossRef](#)]
58. Wang, S.; Gao, S.; Huang, Y.; Shi, C. Spatiotemporal Evolution of Urban Carbon Emission Performance in China and Prediction of Future Trends. *J. Geogr. Sci.* **2020**, *30*, 757–774. [[CrossRef](#)]
59. Mu, X.; Fang, C.; Yang, Z. Spatio-Temporal Evolution and Dynamic Simulation of the Urban Resilience of Beijing-Tianjin-Hebei Urban Agglomeration. *J. Geogr. Sci.* **2022**, *32*, 1766–1790. [[CrossRef](#)]
60. Wang, K.; Ma, H.; Fang, C. The Relationship Evolution between Urbanization and Urban Ecological Resilience in the Northern Slope Economic Belt of Tianshan Mountains, China. *Sustain. Cities Soc.* **2023**, *97*, 104783. [[CrossRef](#)]
61. Chen, M.; Jiang, Y.; Wang, E.; Wang, Y.; Zhang, J. Measuring Urban Infrastructure Resilience via Pressure-State-Response Framework in Four Chinese Municipalities. *Appl. Sci.* **2022**, *12*, 2819. [[CrossRef](#)]

**Disclaimer/Publisher’s Note:** The statements, opinions and data contained in all publications are solely those of the individual author(s) and contributor(s) and not of MDPI and/or the editor(s). MDPI and/or the editor(s) disclaim responsibility for any injury to people or property resulting from any ideas, methods, instructions or products referred to in the content.